

Geology

Speleothems and mountain uplift

Michael C. Meyer, Robert A. Cliff and Christoph Spötl

Geology 2011;39;447-450
doi: 10.1130/G31881.1

Email alerting services

click www.gsapubs.org/cgi/alerts to receive free e-mail alerts when new articles cite this article

Subscribe

click www.gsapubs.org/subscriptions/ to subscribe to *Geology*

Permission request

click <http://www.geosociety.org/pubs/copyrt.htm#gsa> to contact GSA

Copyright not claimed on content prepared wholly by U.S. government employees within scope of their employment. Individual scientists are hereby granted permission, without fees or further requests to GSA, to use a single figure, a single table, and/or a brief paragraph of text in subsequent works and to make unlimited copies of items in GSA's journals for noncommercial use in classrooms to further education and science. This file may not be posted to any Web site, but authors may post the abstracts only of their articles on their own or their organization's Web site providing the posting includes a reference to the article's full citation. GSA provides this and other forums for the presentation of diverse opinions and positions by scientists worldwide, regardless of their race, citizenship, gender, religion, or political viewpoint. Opinions presented in this publication do not reflect official positions of the Society.

Notes

Speleothems and mountain uplift

Michael C. Meyer^{1*}, Robert A. Cliff², and Christoph Spötl¹

¹Institut für Geologie und Paläontologie, Universität Innsbruck, Innrain 52, 6020 Innsbruck, Austria

²School of Earth and Environment, University of Leeds, Leeds, LS2 9JT, UK

ABSTRACT

Ancient speleothems were recovered from caves that today are situated in a high-alpine cirque landscape at 2500 m altitude at the northern rim of the European Alps. U-Pb ages date speleothem deposition to the early Quaternary (between 2.16 and 2.12 Ma and ca. 2.00 Ma), i.e., well before the onset of major alpine and Northern Hemisphere glaciations. Using a stable isotope-based modeling approach, we quantitatively estimate the paleoelevation of both the caves and their former catchment area, which in turn allows us to calculate rates of rock and surface uplift (and hence erosion) since 2 Ma. We show that for the frontal part of the Alps, rates of rock uplift and erosion were ~0.75 and ~0.5 mm/yr, respectively, and further suggest that isostatic uplift of mountain peaks of as much as ~500 m in response to enhanced glacial erosion occurred during the Quaternary. This study highlights the potential of U-Pb-dated speleothems for reconstructing paleoaltimetry, particularly in calcareous mountain ranges, where a standard thermochronologic assessment of exhumation and erosion is generally not feasible.

INTRODUCTION

The effect and relative importance of climate and climate change for the evolution of mountain ranges are subjects of ongoing and intense debate (e.g., Kohn, 2007; Whipple, 2009; Egholm et al., 2009). While horizontal shortening of tectonic plates thickens the buoyant crust and elevates the Earth's surface, erosion of such tectonically accreted belts produces relief and triggers isostatic rebound until equilibrium is reached (Whipple, 2009; Tomkin and Roe, 2007). Late Cenozoic climate deterioration and in particular the marked climate variability during the Quaternary significantly enhanced erosional unloading (Peizhen et al., 2001), with profound consequences for the morphotectonic evolution of many active orogens (Berger et al., 2008; Champagnac et al., 2007). Hence, reliable estimates of the interrelated processes of rock uplift, surface uplift, and erosion are highly desirable but difficult to obtain for the Quaternary and often remain poorly constrained (England and Molnar, 1990), especially for calcareous mountain ranges where standard thermochronological techniques are usually not applicable.

U-Pb dating opens up new vistas for paleoenvironmental research, as no upper dating limit is encountered with this radiometric technique, but has been successfully applied to only a handful of speleothems. Here we present data for 2-m.y.-old speleothems dated via the U-Pb isochron technique, which were recovered from fossil caves in the Allgäu Mountains, a segment of the Northern Calcareous Alps in western Austria (Fig. 1). Substantial shortening during the Cretaceous–Tertiary alpine orogeny resulted in a fold-and-thrust belt characterized by south-

southeast-dipping thrust sheets and associated north-northwest-vergent folds (Fig. 1B). As a result, the dolomite host rock reveals steeply dipping bedding planes and axial plane foliation as well as sets of conjugate fractures and faults (Fig. 1C). Intensive glacial erosion during the Quaternary is evidenced by a distinctive cirque landscape (mean peak elevation of ~2500 m), as well as main valleys with U-shaped cross profiles. Due to the position at the northern rim of the Alps, the Allgäu Mountains are directly

exposed to the northwesterlies and receive as much as 2500 mm of mean annual precipitation, making this Northern Calcareous Alps segment one of the wettest places both north of the Alps and of the entire orogen (Frei and Schär, 1998). Two caves are located at ~2450 m in cirque walls of the Allgäu main crest (Fig. 1B) and host speleothems with high U contents (4–43 ppm) coupled with low nonradiogenic Pb levels, i.e., ideal candidates for the U-Pb isochron technique (Richards et al., 1998). The petrographic and isotopic characteristics of these samples call for environmental and climatic conditions during speleothem formation vastly different from those of today, and are discussed in the following.

RESULTS

Brownish stalagmites and flowstone samples, some in situ, were recovered from the caves; flowstone data were discussed by Meyer et al. (2009). Here we focus on a 36-cm-long candle-shaped stalagmite from the Wilder Mann cave (sample WM5). Four U-Pb ages were determined; these decrease in stratigraphic order from 2.16 +0.02/–0.02 to 2.00 +0.02/–0.07 Ma (2 σ errors; details on the U and Pb isotopic data

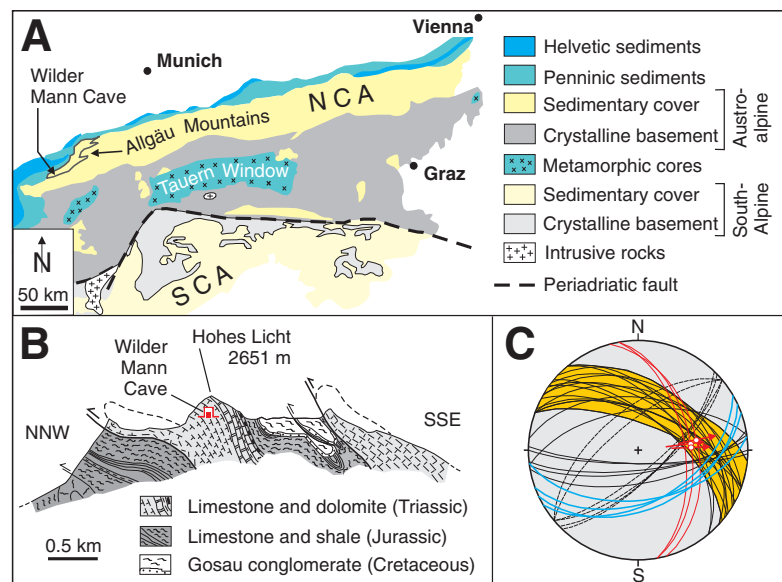


Figure 1. Geological setting of investigation area. A: Tectonic map of Eastern Alps. NCA—Northern Calcareous Alps; SCA—Southern Calcareous Alps. **B:** Geological cross section through main crest of Allgäu Mountains (modified from von Hüffel et al., 1965). **C:** Equal-area stereographic projection (lower hemisphere) from Wilder Mann (WM) cave: blue—bedding planes; yellow—fractures sealed by the 2 m.y. old WM1 flowstone (Meyer et al., 2009); black—axial plane foliation; black dashed—fractures due to relaxation of cirque wall; red—neotectonic fault displacing cave wall.

*E-mail: michael.meyer@uibk.ac.at.

are given in the GSA Data Repository¹). Stalagmite WM5 is characterized by a regular macroscopic lamination and preserves microscopic ultraviolet (UV) fluorescent laminae (~30–70 μm) similar to the UV lamination in the adjacent 2 Ma WM1 flowstone (Meyer et al., 2009), although much fainter. At 60 mm below the top the stalagmite reveals a hiatus. A low-amplitude, low-frequency O isotope signal was obtained for a 30-cm-long sequence between the hiatus and the base of the stalagmite (i.e., growth period 1, $\delta^{18}\text{O}$ mean -11.8‰ , $\delta^{18}\text{O}$ minima -12.5‰ ; Fig. 2). This growth period reveals long-term trends in $\delta^{18}\text{O}$, whereas the $\delta^{13}\text{C}$ values stay almost invariant ($\sim -4\text{‰}$). We checked the WM5 record for isotopic equilibrium conditions via a series of Hendy tests performed along both the stalagmite growth axis and single growth layers. No $\delta^{18}\text{O}/\delta^{13}\text{C}$ covariation was found for growth period 1 ($\Delta\delta^{13}\text{C}/\Delta\delta^{18}\text{O}$ slope = 0.12, $r^2 = 0.03$), whereas simultaneous enrichment of $\delta^{18}\text{O}$ and $\delta^{13}\text{C}$ during growth period 2 ($\Delta\delta^{13}\text{C}/\Delta\delta^{18}\text{O}$ slope = 1.20, $r^2 = 0.34$) is indicative of kinetic isotopic fractionation (Hendy, 1971; Mickler et al., 2006; Fig. 2). The Hendy tests for growth period 1, however, suggest that $\delta^{18}\text{O}$ in cave calcite ($\delta^{18}\text{O}_{\text{cc}}$) reflects the O isotopic composition of the former cave drip water, and thus the meteoric precipitation that fell above the cave ($\delta^{18}\text{O}_{\text{ppt}}$; lamina-parallel Hendy tests in Figure DR2 in the Data Repository). The $\delta^{13}\text{C}$ values in growth period 1 are high and, analogous to modern caves in alpine settings, suggest a small contribution of soil-derived C and a thick rock overburden. The continuous microscopic UV lamination indicates the presence of some soil and vegetation in the infiltration area above the cave, giving rise to a flux of fluorescent organic matter into the karst aquifer during late summer and autumn, when decaying organic material is readily available (Frisia et al., 2003).

ISOTOPIC MODELING

Isotopic equilibrium conditions in growth period 1 of stalagmite WM5 are associated with $\delta^{18}\text{O}_{\text{cc}}$ values of $\sim -12\text{‰}$ to -12.5‰ , and similar findings apply to the adjacent WM1 flowstone (U-Pb dated to 2.02 \pm 0.04/–0.07 Ma), where isotopic equilibrium conditions are manifested by $\delta^{18}\text{O}_{\text{cc}}$ values of $\leq -12\text{‰}$ (Meyer et al., 2009). These values are surprisingly low, i.e., 3‰–4‰ lower than of Holocene speleothems in similar settings (i.e., north alpine caves with catchments between 1500 and 2000 m; Spötl's unpublished data). We also calculated a theoretical $\delta^{18}\text{O}_{\text{cc}}$

¹GSA Data Repository item 2011146, U and Pb isotopic data and methodology, Table DR1, and Figures DR1–DR4, is available online at www.geosociety.org/pubs/ft2011.htm, or on request from editing@geosociety.org or Documents Secretary, GSA, P.O. Box 9140, Boulder, CO 80301, USA.

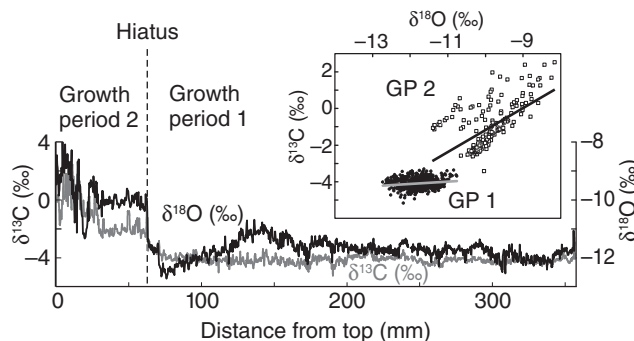


Figure 2. Stable oxygen and carbon isotope record of Wilder Mann cave stalagmite WM5. Inset: Cross-correlation of isotope data retrieved along central growth axis; GP1—growth period 1; GP2—growth period 2.

value for the modern altitude setting of the Allgäu caves. Under isotopic equilibrium $\delta^{18}\text{O}_{\text{cc}}$ is a function of $\delta^{18}\text{O}_{\text{ppt}}$ and the cave temperature (T_c), which in turn reflects the mean annual air temperature (MAAT) outside the cave (Wigley and Brown, 1976). Modern $\delta^{18}\text{O}_{\text{ppt}}$ and T_c values were obtained via extrapolating data from nearby meteorological stations (Table 1; Fig. DR3) and a theoretical $\delta^{18}\text{O}_{\text{cc}}$ value of close to -10‰ was obtained. Note that calcite does not form under these conditions today (MAAT $< 0^\circ\text{C}$; Table 1) and that modern drip water is undersaturated with calcite, and hence corrodes speleothems. In order to explain the unusually low $\delta^{18}\text{O}_{\text{cc}}$ values, changes in paleoelevation and climate have to be invoked and are quantified using a simple isotope model. The model is based on linear calibrations of the local lapse

rates of T_c and $\delta^{18}\text{O}_{\text{ppt}}$ (Fig. DR3), whereby calcite precipitation is treated as an equilibrium process. Because the O isotopic fractionation between calcite and water is temperature dependent ($-0.24\text{‰}/^\circ\text{C}$; Friedman and O'Neil, 1977), the isotopic composition of speleothem calcite formed at lower elevation can be simulated by increasing T_c (via the T lapse rate). The paleoelevation of the infiltration area is varied via the isotopic lapse rate. A range of possible uplift and erosion scenarios is considered by assuming different paleoelevations for the cave and its corresponding catchment (Fig. 3; Table 1). The first set of calculations (scenarios A–D2) assumes that both lapse rate and climate 2 m.y. ago were broadly comparable to today. While scenarios C and D2 come close to the measured $\delta^{18}\text{O}_{\text{cc}}$ values ($\delta^{18}\text{O}_{\text{cc}}$ equilibrium field; Fig. 3),

TABLE 1. PARAMETER SETTINGS AND RESULTS OF THE ISOTOPE MODEL

Scenarios	Modern	A	B	C	D1	D2
Catchment altitude (m)	2500	1500	1500	2000	2500	2500
Cave altitude (m)	2450	500	1000	1000	1000	1500
Catchment temperature ($^\circ\text{C}$)	-1.8 ± 0.3	3.6 ± 0.3	3.6 ± 0.3	1.1 ± 0.3	-1.8 ± 0.3	-1.8 ± 0.3
Cave temperature ($^\circ\text{C}$)	-1.8 ± 0.3	8.1 ± 0.3	5.9 ± 0.3	5.9 ± 0.3	5.9 ± 0.3	3.3 ± 0.3
Catchment $\delta^{18}\text{O}_{\text{ppt}}$ (‰)	-14.2 ± 0.2	-12.4 ± 0.2	-12.4 ± 0.2	-13.3 ± 0.3	-14.2 ± 0.2	-14.2 ± 0.2
Calcite $\delta^{18}\text{O}$ (‰)	n.a.	-10.6 ± 0.3	-10.16 ± 0.3	-11.0 ± 0.3	-11.9 ± 0.3	-11.2 ± 0.3
Rock uplift (mm/yr)	n.a.	1	0.75	0.75	0.75	0.5
Surface uplift (mm/yr)	n.a.	0.5	0.5	0.25	0	0
Erosion (mm/yr)	n.a.	0.5	0.25	0.5	0.75	0.5

Note: Different rates of rock and surface uplift and erosion (implicitly built into each scenario of Fig. 3) are summarized here. Surface uplift (rock uplift) is the displacement of the Earth's surface (of rocks) with respect to the geoid. Erosion is the difference between surface and rock uplift (England and Molnar, 1990). n.a.—not applicable.

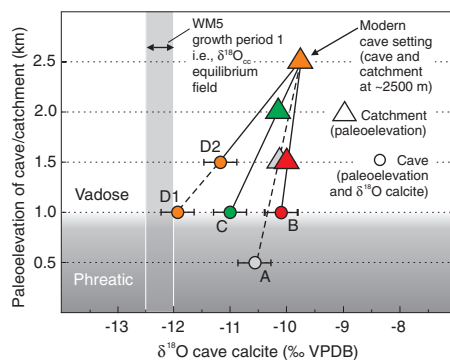


Figure 3. Isotopic modeling of different paleoelevations of cave (Wilder Mann cave, WM) and catchment area. Starting points are modern cave temperature (T_c) and the modern value for $\delta^{18}\text{O}_{\text{ppt}}$ (see Table 1). Isotope model searches for those combinations of parameters $\delta^{18}\text{O}_{\text{ppt}}$ and T_c that permit cave calcite with $\delta^{18}\text{O}$ values as low as -12‰ to -12.5‰ to precipitate. Broken lines indicate scenarios that were discarded based on speleological arguments (discussed in text). VPDB—Vienna Peedee belemnite.

only scenario D1 intersects it; i.e., a combination of a deep-seated cave and an alpine infiltration area (i.e., ≥ 2000 m in altitude) is required to obtain $\delta^{18}\text{O}_{\text{cc}}$ values that approach the measured calcite values of -12‰ to -12.5‰ . A thickness of 1000 m for the vadose zone (scenarios C and D2) is a high value but not uncommon in the Alps (Bauer, 1969), and we suggest that the structural predisposition of the host rock (Fig. 1) allows for efficient transmission of the hydrological surface signal into the underground and that the model of a deep-seated cave can therefore be reconciled with the presence of seasonal laminae (requiring seasonal, organic-bearing karst water pulses to reach the cave). However, a rock overburden of 1500 m, as suggested in scenario D1, appears unrealistically thick and is rarely observed in alpine cave settings today and would probably cause the organic surface signal (responsible for precipitating fluorescent calcite bands during late summer–autumn) to be eliminated by dispersion and mixing en route through such a very thick unsaturated zone (Frisia et al., 2003). Scenario D1 is therefore deemed improbable. Furthermore, the studied speleothems are vadose features and cannot form below the groundwater table, which is at 800–1100 m today; we therefore discard scenario A (cave at 500 m above sea level).

We also investigated the impact of climate-induced temperature changes on $\delta^{18}\text{O}_{\text{cc}}$ (in addition to temperature changes associated with different paleoelevations of the cave) by exploiting the well-established modern relationship between T and $\delta^{18}\text{O}_{\text{ppt}}$ in Central Europe ($0.59\text{‰} \pm 0.08\text{‰}/\text{°C}$; Rozanski et al., 1992). Cooler climatic conditions during calcite precipitation therefore translate into more negative $\delta^{18}\text{O}_{\text{cc}}$ values, and we superimpose this effect on the previously accepted scenarios (B, C, and D2; Fig. 4A). Substantial atmospheric cooling is necessary to meet the isotopic constraints of the Allgäu speleothems (e.g., to 6°C for scenario B), but at the same time the MAAT in the infiltration area plunges below the freezing point (Fig. 4A). This would inevitably initiate periglacial processes and glaciation in the catchment, in stark contrast to the calcite petrography (i.e., the regular UV lamination, the lack of corrosion features and detrital material) and the pollen content from a 2 m.y. old flowstone sample from the same cave (Meyer et al., 2009), all indicating a vegetated and geomorphologically stable infiltration area. Note that scenarios with catchments higher than today (i.e., >2500 m) also result in glacial and periglacial conditions (even without cooling), a strong argument against Northern Calcareous Alps paleoelevations >2500 m 2 m.y. ago. Other mechanisms that could account for the low $\delta^{18}\text{O}_{\text{cc}}$ values include (1) the amount effect (i.e., partial reevaporation of raindrops falling through dry air), and

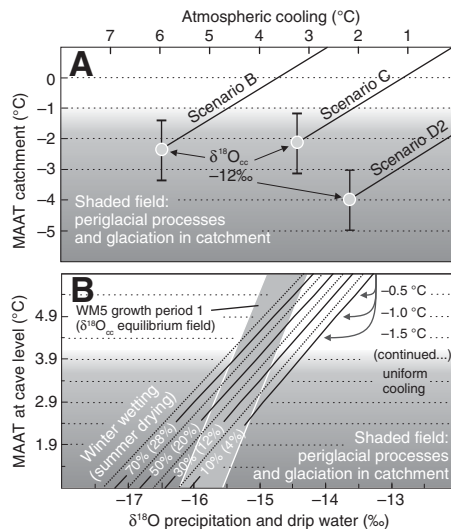


Figure 4. Impact of different climates on isotope model. Atmospheric cooling (A) and seasonality effects (B) are superimposed onto previously accepted scenarios. Gray circles in A indicate amount of cooling required to precipitate $\delta^{18}\text{O}_{\text{cc}}$ values as low as -12‰ to -2.5‰ , while MAAT (mean annual air temperature) in catchment is monitored. In B, only most plausible seasonality solution is shown (i.e., scenario C). WM—Wilder Mann cave.

(2) the possibility that the air masses that delivered moisture to the Northern Calcareous Alps 2 m.y. ago followed very different trajectories compared to today. The amount effect has not been observed in the Alps (despite a dense network of measurement stations), and there is no evidence to suggest a fundamentally different moisture delivery pattern from the Atlantic to the Alps than that of today (Bartoli et al., 2005; Lisiecki and Raymo, 2005). We therefore argue that a more viable mechanism to reconcile the measured $\delta^{18}\text{O}_{\text{cc}}$ values with our most plausible uplift scenarios (C and D2) is seasonal changes in precipitation. The importance of seasonality changes has been demonstrated previously for the Pliocene-Pleistocene transition (Klotz et al., 2006), as well as for late Pleistocene speleothems in the Alps (Meyer et al., 2008), and is exemplified in Figure 4B. Increasing the isotopically light winter precipitation (e.g., in scenario C) by 30% in combination with slightly dryer summers and an atmospheric cooling of $1\text{--}2\text{°C}$ decreases the $\delta^{18}\text{O}_{\text{cc}}$ value by $\sim 1\text{‰}$ and the $\delta^{18}\text{O}_{\text{cc}}$ equilibrium constraints are met (stronger seasonality changes are required for scenario D2 while no intersection with the $\delta^{18}\text{O}_{\text{cc}}$ equilibrium field was achieved for scenario B; Fig. DR4). We favor scenario C over scenario D2, considering the proximity to the glaciation threshold of the latter scenario and the consequential type and magnitude of seasonality changes required to approach the equilibrium $\delta^{18}\text{O}_{\text{cc}}$ values of the WM5 stalagmite.

DISCUSSION AND CONCLUSIONS

The isotopic modeling results are robust and not affected by kinetic isotope fractionation effects that undoubtedly played a role during growth period 2 of stalagmite WM5. The basic assumption in our model is that the temperature lapse rate as well as the isotope lapse rate 2 m.y. ago (and thus upwind rainout patterns; Galewsky, 2009) were broadly comparable to today. This view is supported by paleoenvironmental data suggesting that interglacials during the early Quaternary were constrained by roughly the same climatic boundary conditions as during the Holocene (Bartoli et al., 2005; Lisiecki and Raymo, 2005; Klotz et al., 2006).

The isotope model suggests an alpine infiltration area (2000–2500 m), a deep-seated cave (~ 1000 -m-thick vadose zone), and a seasonality pattern slightly different from those of today. These results are corroborated by (1) palynological data from the adjacent WM1 flowstone, where pollen point toward an alpine infiltration area with only local tree stands, cool-humid summers, and mild winters (Meyer et al., 2009), and (2) the high $\delta^{13}\text{C}$ values of the WM5 stalagmite (requiring a thick rock overburden and a thin soil cover). Rock uplift rates of 0.5 and 0.75 mm/yr are derived from scenarios C and D2, respectively. Both scenarios suggest erosion rates of 0.5 mm/yr. However, 500 m of surface uplift (at a rate of 0.25 mm/yr) is associated with scenario C, whereas surface uplift is balanced by erosion in scenario D2. Considering the position at the northern rim of the Eastern Alps, both rock uplift and erosion rates are high and only comparable in magnitude to rates derived from fission track and sediment budget data closer to the core of the orogen (Kuhlemann et al., 2002; Rahn, 2001).

The past 2 m.y. (i.e., the integration interval for our isotope model) were dominated by glacial valley incision and relief production in many mountain ranges (e.g., Shuster et al., 2005), including the Alps (Häuselmann et al., 2007). Glacial erosion is known to entail isostatic uplift of mountain peaks (Whipple et al., 1999), and we therefore attribute the surface uplift in scenario C to isostatic compensation in response to enhanced glacial unloading during the Quaternary. The alternative mechanism, i.e., uplift of mountain peaks in response to enhanced crustal shortening, is unsubstantiated given the fact that the convergence in the European Alps has declined since the Late Miocene (e.g., Schmid et al., 1996), while alpine erosion rates have increased significantly since ca. 3 Ma (Kuhlemann et al., 2002). Furthermore, analytical models that examine the coupling between glacial erosion and orogen development suggest that erosion and hence rock uplift rates not only are linked to the distribution of precipitation, but relate linearly to the precipitation rate and

are highest at the edges of a glaciated mountain range (Tomkin and Roe, 2007). This view is consistent with our isotopic modeling results and with meteorological (Frei and Schär, 1998) and paleoglacier data (Fiebig et al., 2004) from the Alps. Quaternary landscape evolution at steady state (Egholm et al., 2009) follows from scenario D2 (rock uplift equals erosion), while isostatic peak uplift of ~500 m, probably in response to enhanced glacial erosion, is suggested by scenario C (our favored scenario, as outlined herein). Scenario C is therefore in line with geophysical modeling results from the Western Alps suggesting that Quaternary erosion-induced isostatic rebound was ~500 m (Champagnac et al., 2007).

While thermochronological techniques have been used to study the crystalline core of the alpine orogen, the morphotectonic evolution of its sedimentary peripheral segments has hitherto been much more difficult to constrain. The rims of this orogen are characterized by focused precipitation and erosion, and we pinpointed significant rates for rock uplift and erosion for the Quaternary in one of the northernmost mountain segments. Our study highlights the potential for constraining paleotopography and mountain belt evolution using ancient U-Pb-dated speleothems.

ACKNOWLEDGMENTS

This research was funded by the Austrian Science Fund grant Y122-GEO to Spötl. Geochronological facilities were supported by the University of Leeds and Natural Environment Research Council grant NER/H/S/2000/00853. Meyer was funded by the Seventh Framework Programme of the European Union (grant IOF-GEOPAL-219944) during the writing stage. We thank H. Ortner and B. Fügenschuh for discussion and the referees for helpful comments.

REFERENCES CITED

- Bartoli, G., Sarnthein, M., Weinelt, M., Erlenkeuser, H., Garbe-Schonberg, D., and Lea, D.W., 2005, Final closure of Panama and the onset of Northern Hemisphere glaciation: *Earth and Planetary Science Letters*, v. 237, p. 33–44, doi: 10.1016/j.epsl.2005.06.020.
- Bauer, F., 1969, Karsthydrologische Untersuchungen im Schneepalmenstollen in den steirischen-niederösterreichischen Kalkalpen: *Steirische Beiträge zur Hydrogeologie*, v. 21, p. 193–214.
- Berger, A.L., Gulick, S.P.S., Spotl, J.S., Upton, P., Jaeger, J.M., Chapman, J.B., Worthington, L.A., Pavlis, T.L., Ridgway, K.D., Willems, B.E., and McAleer, R.J., 2008, Quaternary tectonic response to intensified glacial erosion in an orogenic wedge: *Nature Geoscience*, v. 1, p. 793–799, doi: 10.1038/ngeo334.
- Champagnac, J.D., Molnar, P., Anderson, R.S., Sue, C., and Delcou, B., 2007, Quaternary erosion-induced isostatic rebound in the western Alps: *Geology*, v. 35, p. 195–198, doi: 10.1130/G23053A.1.
- Egholm, D.L., Nielsen, S.B., Pedersen, V.K., and Lesemann, J.-E., 2009, Glacial effects limiting mountain height: *Nature*, v. 460, p. 884–887, doi: 10.1038/nature08263.
- England, P., and Molnar, P., 1990, Surface uplift, uplift of rocks, and exhumation of rock: *Geology*, v. 18, p. 1173–1177, doi: 10.1130/0091-7613(1990)018<1173:SUORA>2.3.CO;2.
- Fiebig, M., Buitter, S., and Ellwanger, D., 2004, Pleistocene glaciations of southern Germany, in Ehlers, J., and Gibbard, P., eds., *Quaternary glaciations—Extent and chronology, Part 1: Europe*: Amsterdam, Elsevier, p. 147–154.
- Frei, C., and Schär, C., 1998, A precipitation climatology of the Alps from high-resolution rain-gauge observations: *International Journal of Climatology*, v. 18, p. 873–900, doi: 10.1002/(SICI)1097-0088(19980630)18:8<873::AID-JOC255>3.0.CO;2-9.
- Friedman, I., and O'Neil, J.R., 1977, Compilation of stable isotope fractionation factors of geochemical interest, in Fleischer, M., ed., *Data of geochemistry*: U.S. Geological Survey Professional Paper 440-KK, p. 1–12.
- Frisia, S., Borsato, A., Preto, N., and McDermott, F., 2003, Late Holocene annual growth in three Alpine stalagmites records the influence of solar activity and the North Atlantic Oscillation on winter climate: *Earth and Planetary Science Letters*, v. 216, p. 411–424, doi: 10.1016/S0012-821X(03)00515-6.
- Galewsky, J., 2009, Orographic precipitation isotopic ratios in stratified atmospheric flows: Implications for paleoelevation studies: *Geology*, v. 37, p. 791–794, doi: 10.1130/G30008A.1.
- Häuselmann, P., Granger, D.E., Jeannine, P.Y., and Lauritzen, S.E., 2007, Abrupt glacial valley incision at 0.8 Ma dated from cave deposits in Switzerland: *Geology*, v. 35, p. 143–146, doi: 10.1130/G23094A.
- Hendy, C.H., 1971, The isotopic geochemistry of speleothems. 1. The calculation of the effects of the different modes of formation on the isotopic composition of speleothems and their applicability as palaeoclimatic indicators: *Geochimica et Cosmochimica Acta*, v. 35, p. 801–824, doi: 10.1016/0016-7037(71)90127-X.
- Klotz, S., Fauquette, S., Combourieu-Nebout, N., Uhl, D., Suc, J.P., and Mosbrugger, V., 2006, Seasonality intensification and long-term winter cooling as a part of the late Pliocene climate development: *Earth and Planetary Science Letters*, v. 241, p. 174–187, doi: 10.1016/j.epsl.2005.10.005.
- Kohn, M.J., 2007, Paleoaclimetry: Geochemical and thermodynamic approaches: *Reviews in Mineralogy and Geochemistry* 66, 278 p.
- Kuhlemann, J., Frisch, W., Szekely, B., Dunkl, I., and Kazmer, M., 2002, Post-collisional sediment budget history of the Alps: Tectonic versus climatic control: *International Journal of Earth Sciences*, v. 91, p. 818–837, doi: 10.1007/s00531-002-0266-y.
- Lisiecki, L.E., and Raymo, M.E., 2005, A Pliocene-Pleistocene stack of 57 globally distributed benthic $\delta^{18}\text{O}$ records: *Paleoceanography*, v. 20, PA1003, doi: 10.1029/2004PA001071.
- Meyer, M.C., Spötl, C., and Mangini, A., 2008, The demise of the Last Interglacial recorded in isotopically dated speleothems from the Alps: *Quaternary Science Reviews*, v. 27, p. 476–496, doi: 10.1016/j.quascirev.2007.11.005.
- Meyer, M.C., Cliff, R.A., Spötl, C., Knipping, M., and Mangini, A., 2009, Speleothems from the earliest Quaternary: Snapshots of paleoclimate and landscape evolution at the northern rim of the Alps: *Quaternary Science Reviews*, v. 28, p. 1374–1391, doi: 10.1016/j.quascirev.2009.01.010.
- Mickler, P.J., Stern, L.A., and Banner, J.L., 2006, Large kinetic isotope effects in modern speleothems: *Geological Society of America Bulletin*, v. 118, p. 65–81, doi: 10.1130/B25698.1.
- Peizhen, Z., Molnar, P., and Downs, W.R., 2001, Increased sedimentation rates and grain sizes 2–4 Myr ago due to the influence of climate change on erosion rates: *Nature*, v. 410, p. 891–897, doi: 10.1038/35073504.
- Rahn, M., 2001, The metamorphic and exhumation history of the Helvetic Alps, Switzerland, as revealed by apatite and zircon fission tracks [habilitation thesis]: Freiburg, Germany, Albert-Ludwigs-Universität Freiburg, 140 p.
- Richards, D.A., Bottrell, S.H., Cliff, R.A., Ströbe, K., and Rowe, P.J., 1998, U-Pb dating of Quaternary-age speleothem: *Geochimica et Cosmochimica Acta*, v. 62, p. 3683–3688, doi: 10.1016/S0016-7037(98)00256-7.
- Rozanski, K., Araguás-Araguás, L., and Gonfiantini, R., 1992, Relation between long-term trends in oxygen-18 isotope composition of precipitation and climate: *Science*, v. 258, p. 981–985, doi: 10.1126/science.258.5084.981.
- Schmid, S.M., Pfiffner, O.A., Froitzheim, N., Schönborn, G., and Kissling, E., 1996, Geophysical-geological transect and tectonic evolution of the Swiss-Italian Alps: *Tectonics*, v. 15, p. 1036–1064, doi: 10.1029/96TC00433.
- Shuster, D.L., Ehlers, T.A., Rusmoren, M.E., and Farley, K.A., 2005, Rapid glacial erosion at 1.8 Ma revealed by $^4\text{He}/^3\text{He}$ thermochronometry: *Science*, v. 310, p. 1668–1670, doi: 10.1126/science.1118519.
- Tomkin, J.H., and Roe, G.H., 2007, Climate and tectonic controls on glaciated critical-taper orogens: *Earth and Planetary Science Letters*, v. 262, p. 385–397, doi: 10.1016/j.epsl.2007.07.040.
- von Hückel, B., Jacobshagen, V., and Stengel-Rutkowski, W., 1965, Über den Bau des Allgäuer Hauptkammes und der Hornbachkette (Nördliche Kalkalpen): *Zeitschrift der Deutschen Geologischen Gesellschaft*, v. 112, p. 91–104.
- Whipple, K.X., 2009, The influence of climate on the tectonic evolution of mountain belts: *Nature Geoscience*, v. 2, p. 97–104, doi: 10.1038/ngeo413.
- Whipple, K.X., Kirby, E., and Brocklehurst, S.H., 1999, Geomorphic limits to climate-induced increases in topographic relief: *Nature*, v. 401, p. 39–43, doi: 10.1038/43375.
- Wigley, T.M.L., and Brown, M.C., 1976, The physics of caves, in Ford, T.D., and Cullingford, C.H.D., eds., *The science of speleology*: London, Academic Press, p. 329–358.

Manuscript received 4 November 2010
Manuscript accepted 13 December 2010

Printed in USA